

## Study of thermoelectric cooling characteristics based on measurement data and numerical analysis

© E.N. Vasil'ev

Institute of Computational Modeling, Siberian Branch, Russian Academy of Sciences,  
660036 Krasnoyarsk, Russia  
e-mail: ven@icm.krasn.ru

Received November 1, 2025

Revised November 28, 2025

Accepted December 17, 2025

The results of measurements and calculations of the energy characteristics (cooling capacity and coefficient of performance) of a thermoelectric refrigerator model in air are presented. Heat flux measurements were made using two heat meters located on opposite sides of the thermoelectric module. Numerical analysis of current, voltage, and temperature measurements allowed us to establish the dependence of the cooling capacity and temperature drop across the thermoelectric module on the temperature of its hot side. Experiments determined the energy characteristics of the cooling process over a wide range of operating parameters. Computational modeling of heat transfer processes in the refrigerator model under various operating conditions was conducted; the modeling results are consistent with the measurement data.

**Keywords:** thermoelectric cooling system, heat flux measurement, least-squares method, computational modeling.

DOI: 10.61011/TP.2026.04.63272.302-25

### Introduction

Thermoelectric cooling systems are designed to be applied in various fields of engineering: electronics, space applications, medicine, household appliances, etc. [1–6]. The thermoelectric devices shall be designed and operating modes shall be subsequently effectively controlled with taking into account technical characteristics and parameters of Peltier thermoelectric modules (TEM), which correspond to operation in real conditions. The operating characteristics of the commercial Peltier thermoelectric modules are usually given in accompanying documentation for vacuum and a certain temperature of the hot side [7]. But most often they are operated in air and in this case there are thermal losses originated due to heat exchange between the TEM sides because of mechanisms of thermal conductivity, convection and possible moisture condensation (for unsealed TEMs). Physical properties of the thermoelectric semiconductor materials depend on the temperature and, therefore, the operating characteristics of the thermoelectric modules are also affected by temperature conditions that can vary within wide limits and significantly differ from the values provided in the accompanying technical documentation. Additionally, cooling efficiency is greatly affected by thermal resistances of devices of heat input and removal, wherein intensity of heat exchange of the TEMs with a cooled item and the environment depends on their value [8]. Therefore, designing and operating the thermoelectric cooling systems requires taking into account influence of the said factors on their operating characteristics.

The present study is aimed at investigating influence of the temperature conditions on energy characteristics of the

thermoelectric cooling system in air according to data of measurements and numerical analysis. At the same time, at first, based on the data of the measurements influence of the temperature of the hot side of the TEM on its operating characteristics is determined, which is followed by considering the results of the measurements and the calculations of the characteristics of the thermoelectric cooling system as a whole.

### 1. Description of the experimental bench and the measurement technique

Determination of the TEM operating characteristics, which correspond to the operating conditions, requires additional studies based on measurements and numerical analysis. The experiments for determining the TEM characteristics were performed on a model of a thermoelectric cooler [9]. This model is a thermally insulated housing, which comprises a fan, a heat source and a section of the thermoelectric unit. The heat source (electric heater) was used to vary thermal power input into a cooling chamber and the fan provided circulation of air in a cooled volume. The main functional assembly of the model is the section of the thermoelectric unit, whose layout is drawn in Fig. 1, *a*. The section consists of the commercial thermoelectric module TV-199-1.4-0.8 as well as the devices of heat input and removal. According to the accompanying documentation, this serial thermoelectric module has the highest values of a temperature drop  $\Delta T_{\text{TEM}} = 74^\circ\text{C}$  and cooling capacity  $Q = 191\text{ W}$  at the current  $I_{\text{max}} = 11.8\text{ A}$  and the temperature of the hot side  $T_H = 27^\circ\text{C}$ . Heat was

removed from the thermoelectric module by the liquid aluminum radiator connected to a circulation thermostat. Heat was transferred from a volume of the cooling chamber to the TEM cold side by a heat input device that consisted of three thermosiphons with the common heat distributor with fins of the air heat exchanger strung thereon. The copper heat distributor provides effective heat transfer from the thermosiphons to the TEM cold side.

The experiments included measurement of the values of the temperature  $T$  as well as electrophysical parameters: voltage  $U$  and current  $I$ . The temperature was measured by thermocouples in various points of the device under study. Heat release by the thermoelectric module, the fan and the heat source was determined power supply parameters, wherein the value of  $U$  was measured directly at an input of these devices in order to avoid influence of external losses.

In order to determine the energy characteristics of the cooling system, a value of a heat flux that hits the cold side of the thermoelectric module shall be measured. Various methods and devices are known for measuring the heat fluxes [10–13]. The present study considers steady-state modes, therefore, the heat meter of the auxiliary-wall type was selected for measuring continuous heat fluxes. In this case, it is a plate that is made of an aluminum alloy and has a side contact surface that is equal to that of the thermoelectric module. A density of the heat flux transmitted through the heat meter is calculated by data of thermocouple measurement of the temperature difference  $\Delta T$  at its opposite sides by means of the formula  $q = \lambda \Delta T / \delta$ , where  $\delta$  is a thickness of the plate,  $\lambda$  is a thermal conductivity coefficient of the material. A method error depends on a degree of nonuniformity of distribution of the heat flux over the contact surfaces. In the considered structure of the cooler model the uniformity condition is not fulfilled to a sufficient extent. In the heat distributor and the liquid radiator, heat is transferred on walls of cylindrical channels (Fig. 1, *b*), which causes nonuniformity of fields of the temperature and the heat flux density on side contacting boundaries of these elements of the structure. Besides, the thermocouples in the heat meter are arranged in grooves filled with a thermal paste with a relatively low thermal conductivity coefficient. This configuration disrupts unidimensionality of the problem and results in a need of replacement of the thickness of the heat meter and its thermal conductivity coefficient with certain effective values  $\delta^*$  and  $\lambda^*$ , wherein the heat flux  $Q$  transmitted through the heat meter is written as follows:

$$Q = \lambda^* k^* \frac{\Delta T S}{\delta^*} = k^* \frac{\Delta T}{R}. \quad (1)$$

Here  $k^*$  is a certain coefficient of proportionality,  $S$  is an area of the side surface of the heat meter. Thermal resistance of the heat meter  $R$  primarily depends on its geometric parameters and thermal conductivity coefficients of the material of the plate and the thermal paste [14,15]. It is impossible to reliably calculate  $\delta^*$  and  $\lambda^*$  due to an unknown distribution of a thickness of thermal paste

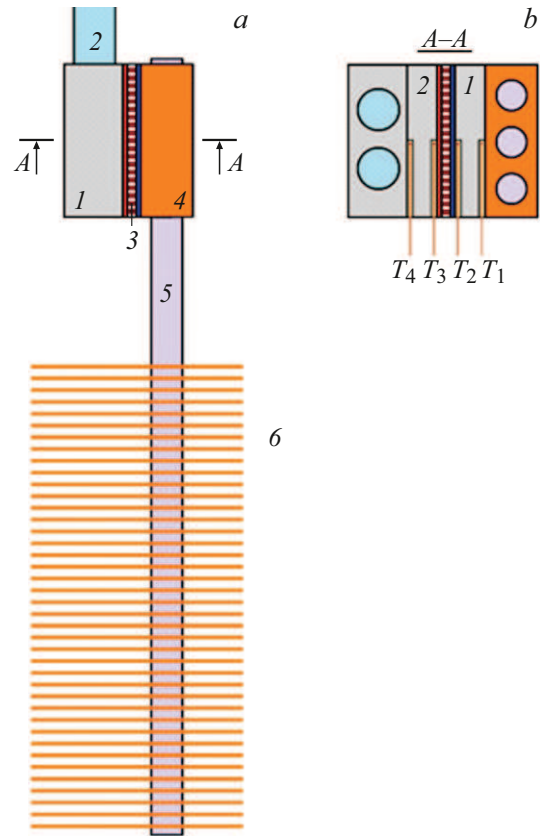


**Figure 1.** Layout diagram: 1 — the liquid radiator, 2 — input of a coolant, 3 — the thermoelectric module, 4 — the heat distributor, 5 — the thermosiphons, 6 — the plates of the air heat exchanger (*a*); arrangement of thermocouples in the heat meters 1 and 2 (*b*).

layers adjacent to thermocouple conductors and their mutual thermal influence.

In order to minimize influence of the above-said adverse factors, we applied a system of two identical heat meters installed on the opposite sides of the thermoelectric module. At the side surfaces of both the heat meters, two thermocouples are installed in the grooves, recording local values of the temperature (Fig. 1, *b*). This differential system of measurement by two heat meters made it possible to exclude physical parameters, whose determination has a significant error. Equations for calculating the heat flux transmitted through the first and second heat meters are written similar to the expression (1):

$$Q = k_1 \frac{T_1 - T_2}{R_1}, \quad (2)$$

$$Q + W = k_2 \frac{T_3 - T_4}{R_2}. \quad (3)$$

Here,  $T_1$  and  $T_2$  are readings of the thermocouples in the first heat meter,  $T_3$  and  $T_4$  are readings of the thermocouples in the second heat meter,  $k_1$  and  $k_2$  are unknown coefficients that illustrate the specifics of each

of the heat meters,  $W = UI$  is electrical power of the thermoelectric module,  $R_1$  and  $R_2$  are thermal resistances of the heat meters 1 and 2. The values of  $R_1$  and  $R_2$  are unknown and their difference is expressed by means of a coefficient  $k_3$ :

$$R_1 = k_3 R_2. \quad (4)$$

From the formulas (2)–(4) we have a relationship for the sought-for heat flux coming to the thermoelectric module:

$$Q = \frac{UI}{k(T_3 - T_4)/(T_1 - T_2) - 1}. \quad (5)$$

Here,  $k = k_2 k_3 / k_1$  is a coefficient that takes into account all specific features of the configuration of the system of measurement with the two heat meters. At the same time, the formula (5) finally includes only the values of  $U$ ,  $I$ ,  $T_1$ ,  $T_2$ ,  $T_3$  and  $T_4$ , which are measured with quite high accuracy, while it omits the parameters that characterize thermal conductivity of the materials and specific features of the geometry of the heat meters.

The value of  $k$  was determined by performing calibration experiments with power supply of the thermoelectric module turned off, wherein  $W = 0$  and the same heat flux is transmitted through the heat meters. Then, taking into account (2)–(4) we obtain the value of  $k = (T_1 - T_2)/(T_3 - T_4)$ , which is determined by data of measurement of local values of the temperature. The calibration experiments are described in the study [16]. The calibration resulted in obtaining an average value  $k = 1.57$ , without detecting an explicit dependence of  $k$  on a value and a direction of  $Q$ . It should be noted that with ideal uniform distribution of the heat flux density the value of  $k$  shall be unity for absolutely identical heat meters.

According to the formula (5), the error of determination of the heat flux depends on accuracy of determination of the coefficient  $k$ , the temperature differences on the heat meters and the electrophysical parameters. In the study [16], a maximum deviation of the coefficient  $k$  from its average value was  $\pm 4.5\%$  with a root-mean-square deviation of  $3.6\%$ . These deviations are due to the error of measurement of the temperature differences for the expression  $k = (T_1 - T_2)/(T_3 - T_4)$ . During pre-calibration of the thermocouples we have found that accuracy of measurement of the local temperature was at least  $0.1^\circ\text{C}$ , while a typical value of the temperature differences in the experiments was  $2^\circ\text{C}$ – $3^\circ\text{C}$ . Accuracy of measurement of current and voltage is much higher than the thermal measurements and does not noticeably affect total accuracy of the technique. Let us estimate influence of the error of determination of the coefficient  $k$  on cooling capacity according to the formula (5). With the TEM turned on, a value of the differences  $T_1 - T_2$  and  $T_3 - T_4$  is directly proportional to the values of thermal power transmitted through the first and second heat meters. Thermoelectric cooling is characterized by a low coefficient of performance. Thus, in the mode of maximum cooling capacity, the coefficient of performance  $\varepsilon = Q/(UI) \approx 0.25$ , wherein

thermal power  $Q + UI \approx 5Q$  is transmitted through the second heat meter. The temperature drop at the heat meters is directly proportional to the value of the heat fluxes. Therefore,  $T_3 - T_4 \approx 5(T_1 - T_2)$  and with substitution the formula (5) is written as  $Q = UI/(5k - 1)$ , and in this case variation of the coefficient  $k$  by  $4.5\%$  will result in a change of  $Q$  by  $4.9\%$ .

Two series of experiments were performed when studying the characteristics of the thermoelectric cooling system. The first series was performed with the heat meters arranged to determine the TEM operating characteristics at the various temperature conditions. The experiments also included determination of thermal resistance of the housing of the cooler model. During this series, in addition to the readings of the thermocouples in the heat meters, also recorded temperatures of air inside the housing ( $T_5$  at an inlet of and  $T_6$  at an outlet of the air radiator) and outside air ( $T_7$ ) were recorded. The values of  $T_2$  and  $T_3$  were considered as a temperature of the cold and the hot sides of the thermoelectric module. Based on the data of measurements of the temperatures and determination of cooling capacity, thermal resistance of the housing of the cooler model was calculated  $R_B = (T_7 - 0.5T_5 - 0.5T_6)/Q = 1.8\text{ K/W}$ . The second series of the experiments included determination of efficiency of the cooler as a whole for the various modes of operation, wherein the heat meters were removed from the structure of the section of the thermoelectric unit, since they are additional thermal resistances that reduce efficiency of thermoelectric cooling. At the same time, the thermocouples for measuring  $T_2$  and  $T_3$  were rearranged in grooves of the heat distributor and the liquid radiator on sides that contact the TEM.

## 2. Measurement of the TEM operating characteristics in air at the various temperature conditions

The investigation of the TEM operating characteristics in air included measurements of the thermal and electrophysical parameters, which made it possible to determine values of the temperatures, heat fluxes, thermal resistances, current and voltage. Based on the results of measurements at the various values of the hot side temperatures  $T_H$ , we have plotted load straight lines  $Q(\Delta T_{\text{TEM}})$  that relate cooling capacity of the TEM to the temperature drop at its sides. Fig. 2 shows load straight lines that correspond to the TEM power supply current  $I = 0.75 \cdot I_{\text{max}} = 8.85\text{ A}$  and the values of the hot side temperature  $T_H = 14^\circ\text{C}$ ,  $20^\circ\text{C}$ ,  $25^\circ\text{C}$ ,  $30^\circ\text{C}$ ,  $35^\circ\text{C}$  and  $40^\circ\text{C}$ . The magnitude  $T_H$  was assumed to be equal to the value of  $T_3$  of the thermocouple that was arranged on the second heat meter and adjacent to the TEM hot side. A lower straight line in the figure refers to  $T_H = 14^\circ\text{C}$ , while a higher one refers to  $T_H = 40^\circ\text{C}$ , and a location of intermediate straight lines subsequently increases with an increase of the hot side temperature, since with the increase of  $T_H$  the higher values of  $Q$  and  $\Delta T_{\text{TEM}}$

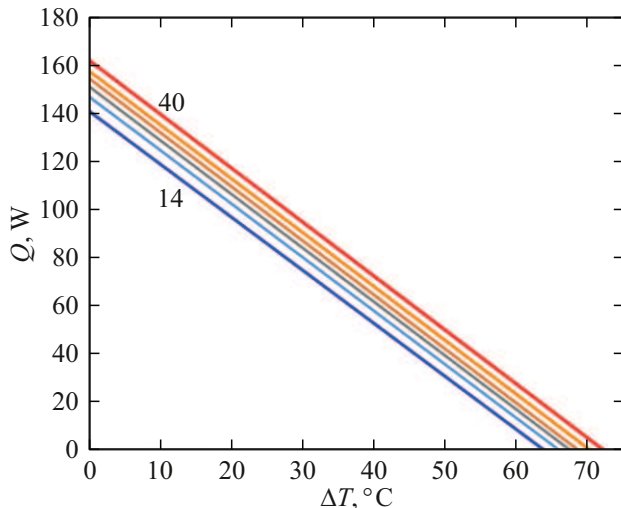


**Figure 2.** Load characteristics with the current  $I = 8.85$  A and the temperature values  $T_H = 14^\circ\text{C}$ ,  $20^\circ\text{C}$ ,  $25^\circ\text{C}$ ,  $30^\circ\text{C}$ ,  $35^\circ\text{C}$  and  $40^\circ\text{C}$ .

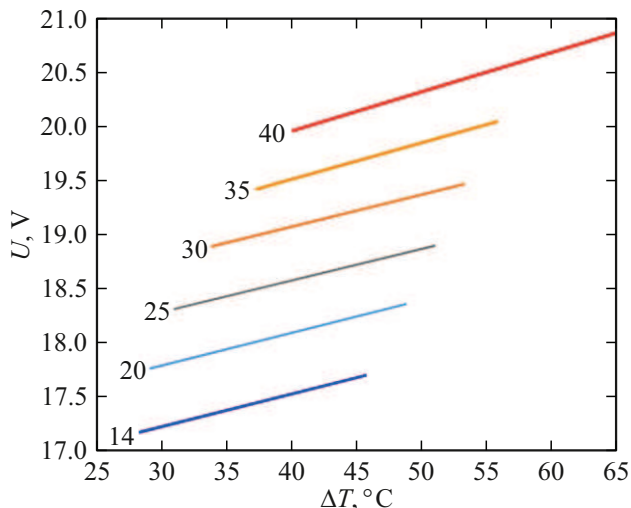


**Figure 3.** Dependences of voltage on the temperature drop at the TEM with the current  $I = 8.85$  A and the temperature values  $T_H = 14^\circ\text{C}$ ,  $20^\circ\text{C}$ ,  $25^\circ\text{C}$ ,  $30^\circ\text{C}$ ,  $35^\circ\text{C}$  and  $40^\circ\text{C}$ .

are attained. The load characteristics have the similar nature at the other values of the current as well.

Another important characteristic that makes it possible to determine a value of intrinsic energy consumption and TEM energy efficiency is a dependence of voltage  $U$  on the temperature conditions. The dependences  $U(\Delta T_{\text{TEM}})$  have been obtained during the same series of measurements at the values of the hot side temperatures  $T_H = 14^\circ\text{C}$ ,  $20^\circ\text{C}$ ,  $25^\circ\text{C}$ ,  $30^\circ\text{C}$ ,  $35^\circ\text{C}$  and  $40^\circ\text{C}$ . Fig. 3 shows them for the current  $I = 0.75 \cdot I_{\text{max}} = 8.85$  A and the values of  $T_H$  are shown in the respective graphs. It is clear from the figure that the magnitude  $U$  proportionally increases with an increase of both  $\Delta T_{\text{TEM}}$  and  $T_H$  and this trend is observed at the other values of the current.

### 3. Determination of the dependence of the TEM operating characteristics on the hot side temperature

In order to calculate and optimize the parameters of the thermoelectric cooling system, it is necessary to specify the TEM operating characteristics for the real temperature conditions of operation. Thus, for the cooling system under study these conditions depend on the TEM operating mode, the values of the temperature of air in the cooling chamber and a room as well as on the temperature of the coolant in the liquid radiator. In the various operation modes, the hot side temperature  $T_H$  can vary within a wide range of the values, which, in turn, affects the TEM operating characteristics. The results of the performed measurements make it possible to determine influence of the hot side temperature of the thermoelectric module on its operating characteristics.

The most informative are extreme point of the load straight lines and they define the maximum values of cooling capacity  $Q$  and the temperature difference  $\Delta T_{\text{TEM}}$ . The maximum values of  $Q$ , which are obtained based on the results of the performed experiments for the studied range of the hot side temperatures  $T_H = 14^\circ\text{C} - 40^\circ\text{C}$  and the three values of the current  $0.25 \cdot I_{\text{max}} = 2.95$  A,  $0.5 \cdot I_{\text{max}} = 5.9$  A and  $0.75 \cdot I_{\text{max}} = 8.85$  A, are marked by squares in Fig. 4. Within the considered range of  $T_H$  the maximum cooling capacity of the TEM at the current  $I = 8.85$  A varies from 141 to 162 W. Based on the obtained maximum values of  $Q$ , the least-square method was used to determine linear functions, which are shown in the figure by solid lines, and numerical values on the straight lines correspond to the values of the current as a percentage of  $I_{\text{max}}$ . Circles in Fig. 4 mark maximum values of cooling capacity  $Q$ , which correspond to technical documentation a TEM manufacturer. The largest difference of about 7% between the calculated values of  $Q$  (152 W when  $T_H = 27^\circ\text{C}$ ) and the manufacturer data (163.5 W) is observed when  $I = 8.85$  A. The smaller value of cooling capacity, which is obtained as a result of the measurements, seems to be primarily caused by thermal losses within the volume of the thermoelectric module during operation in air.

The maximum values of  $\Delta T_{\text{TEM}}$ , which are obtained based on data of the experiments in the studied range  $T_H = 14^\circ\text{C} - 40^\circ\text{C}$  at the values  $I = 0.25 \cdot I_{\text{max}}$ ,  $0.5 \cdot I_{\text{max}}$  and  $0.75 \cdot I_{\text{max}}$ , are shown in Fig. 5 by squares, while the circles mark the values of  $\Delta T_{\text{TEM}}$  from the technical documentation of the thermoelectric module. In this range of  $T_H$ , with the magnitude  $I = 8.85$  A the maximum temperature drop varied from  $63.8^\circ\text{C}$  to  $72.1^\circ\text{C}$ . The straight lines mark the dependences obtained by the experimental values in the least-square method for the three values of the current, whose values are shown in the respective straight lines. For  $I = 8.85$  A and  $T_H = 27^\circ\text{C}$ , the graph-defined value

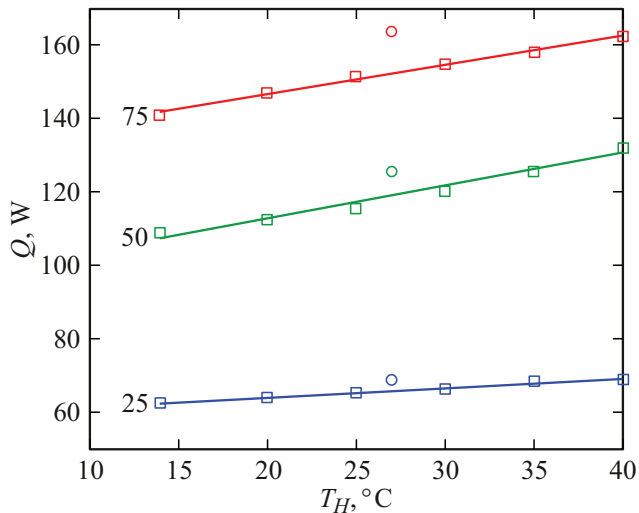


**Figure 4.** Experimental data (squares) and the calculated dependences  $Q_{\max}(T_H)$ , the straight lines include the value of  $I$  as a percentage of  $I_{\max}$ , and the circles mark the values of  $Q_{\max}$ , which are obtained from the TEM technical documentation.

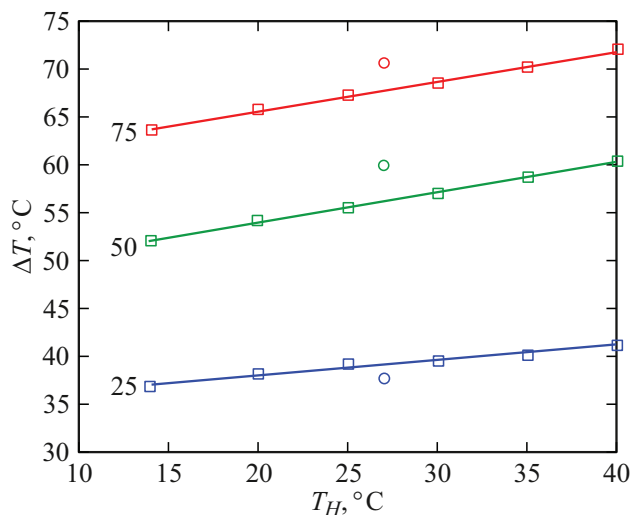


**Figure 5.** Experimental data (squares) and the calculated dependences  $\Delta T_{\max}(T_H)$ , the straight lines include the value of  $I$  as a percentage of  $I_{\max}$ , and the circles mark the values of  $\Delta T_{\max}$ , which are obtained from the technical documentation.

$\Delta T_{\text{TEM}} = 67.9^\circ\text{C}$  is below the manufacturer data ( $70.7^\circ\text{C}$ ) by 4%.

The measured dependences of voltage of thermoelectric module power supply  $U(\Delta T_{\text{TEM}})$ , which are shown in Fig. 3, are obtained for different ranges of the temperature drop. These dependences have a linear increasing form and for numerical analysis they were reduced to a single range of the temperature drop. It included determination of the minimum  $U_{\min}$  (when  $\Delta T_{\text{TEM}} = 30^\circ\text{C}$ ) and maximum  $U_{\max}$  values of voltage (when  $\Delta T_{\text{TEM}} = 55^\circ\text{C}$ ). These minimum (the squares) and maximum (the circles) values are shown in Fig. 6 for the three currents  $I = 0.25 \cdot I_{\max}$ ,  $0.5 \cdot I_{\max}$  and

$0.75 \cdot I_{\max}$ . Based on these values, the least-square method was taken to plot linear-function dependences  $U_{\min}(T_H)$  and  $U_{\max}(T_H)$ , which are shown in the figure by solid straight lines, and for each pair of the graphs the respective values of  $I$  as a percentage of  $I_{\max}$  are given.

Further on, the dependences  $Q(T_H)$ ,  $\Delta T_{\text{TEM}}(T_H)$ ,  $U_{\min}(T_H)$  and  $U_{\max}(T_H)$ , which are obtained as a result of processing of the measurement data, were used when calculating the characteristics of the thermoelectric cooling system in air at the various temperature conditions.

#### 4. Results of measurements and calculations of the energy characteristics of the thermoelectric cooling system

Energy efficiency of the thermoelectric cooler is characterized by two basic parameters: cooling capacity and the coefficient of performance. These parameters for the cooler model have been determined both by direct measurements in the bench during the second series of the experiments and as a result of numerical analysis using the TME operating characteristics obtained in the first series of the experiments.

The second series of the experiments included determination of cooling capacity  $Q$  of the cooler model in a dependence on the TEM power supply current, wherein the specified air temperature of  $+3^\circ\text{C}$  in the cooled volume of the thermoelectric cooler was stabilized by varying power of the heat source. The experiments included recording electrical powers of the fan  $W_1$  and the heat source  $W_2$ , the temperatures of the cold  $T_2$  and the hot side  $T_3$  of the thermoelectric module, air at the inlet  $T_5$  and the outlet of the heat exchanger  $T_6$ , outside air ( $T_7$ ). The data of these temperature measurements were used to calculate the thermal flux through the housing walls  $Q_B = (T_7 - 0.5T_5 - 0.5T_6)/R_B$ . Finally, the magnitude  $Q$  is

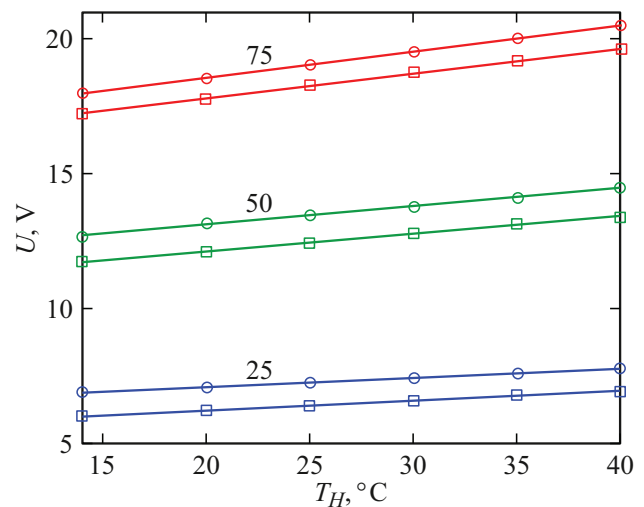


**Figure 6.** Dependences  $U_{\min}(T_H)$  (squares) and  $U_{\max}(T_H)$  (circles) for the values of  $I$  give as a percentage of  $I_{\max}$ .

Values of the measured and the calculated parameters of the cooling system

$I$ , A	$R_T$ , K/W	$R_S$ , K/W	$\Delta T_{\text{TEM}}$ , °C	$Q$ , W	$\varepsilon$
4	0.27	0.1	31.4	28.4	0.732
			32.2	26.7	0.693
5.9	0.281	0.106	40.7	37.5	0.463
			40.7	37.1	0.455
7	0.286	0.107	46	40.2	0.353
			45.7	40.9	0.357
8	0.292	0.108	50.9	42.4	0.283
			50.4	42.6	0.283
8.5	0.292	0.109	53.2	42.4	0.25
			52.8	42.8	0.251
8.85	0.291	0.109	55	42.6	0.229
			54.6	42.7	0.23
9.5	0.289	0.11	58.2	41.4	0.191
			57.8	42	0.194
11	0.282	0.111	65.8	37.9	0.126
			–	–	–
11.4	0.276	0.111	67.8	36.6	0.112
			–	–	–

equal to a sum of thermal powers removed from the cooled volume:

$$Q = W_1 + W_2 + Q_B.$$

Efficiency of thermoelectric cooling significantly depends on thermal resistances of the devices of heat input  $R_T$  and removal  $R_S$ , and the measurement data were used to determine the values  $R_T = (0.5T_5 + 0.5T_6 - T_2)/Q$  and  $R_S = (T_3 - T_8)/(Q + W)$ .

The measured values of the parameters of the cooler model at the coolant temperature  $T_8 = 20^\circ\text{C}$  in the liquid radiator are given in Table for the different current  $I$ . The second and third columns of Table include the thermal resistances of the devices of heat input and removal, upper lines of the cells of the fourth, fifth and sixth columns show measurement-obtained values of the temperature drop  $\Delta T_{\text{TEM}} = T_3 - T_2$ , cooling capacity  $Q$  and the coefficient of performance, which is calculated by means of the relationship  $\varepsilon = Q/(IU)$ .

The measurement-obtained basic values of the main parameters of the cooler model are also shown in Fig. 7. The circles mark cooling capacity  $Q$ , so do the squares the temperature drop  $\Delta T_{\text{TEM}}$  and the crosses the coefficient of performance. With the increase of  $I$ , the studied range exhibits an increase of  $\Delta T_{\text{TEM}}$ , a fall of  $\varepsilon$ , while the magnitude  $Q$  is the highest within the range  $I \approx 8 - 9$  A. Despite stability of the boundary temperature conditions (the values of the temperatures of air inside the cooler housing and the coolant in the liquid radiator), the value of

$T_H = T_3$  significantly varied during the experiments: from  $26.8^\circ\text{C}$  when  $I = 4$  A to  $60.2^\circ\text{C}$  when  $I = 11.4$  A.

Based on the measured TEM operating characteristics, we have calculated the basic parameters of the cooler model. In the ideal case, when there are not thermal losses in heat input and removal, a steady-state temperature drop between a cooled object and the environment will be equal to the thermal module's temperature difference  $\Delta T_0 = -\Delta T_{\text{TEM}}(I, Q, T_H)$ . A negative sign in this expression is caused by the fact that unlike the usual heat-transfer process, the thermoelectric module that functions as a heat pump reversely transfers heat from the cold side to the hot side. The value of the temperature drop is determined by the TEM operation mode, which depends on current  $I$ , transferred thermal power  $Q$  and the hot side temperature  $T_H$ . In the real cooling system, a part of the TEM-produced negative temperature drop is spent to compensate thermal losses in the devices of heat input and removal. The TEM cold side is provided with thermal power  $Q$  by the device of heat input, which has thermal resistance  $R_T$ , therefore, the temperature drop at this device is  $R_T Q$ . In addition to  $Q$ , the device of heat removal transfers Joule heat  $W = UI$  released in the very TEM into the environment. As demonstrated by the measurements, the value of TEM power supply voltage depends on current  $I$ , transferred thermal power  $Q$  and the hot side temperature  $T_H$ . Therefore, the temperature drop that is steady-state at the device of heat removal (the liquid radiator) is  $R_S[Q + U(I, Q, T_H)I]$ . Finally, in order to calculate the characteristics of the thermoelectric cooler model, we write an equation that reflects a balance of the temperature drops taking into account main heat-exchange processes and defines the difference  $\Delta T_0$  between the values of the temperature of air in the cooler housing volume and of the coolant in the liquid radiator

$$\Delta T_0 = R_T Q - \Delta T_{\text{TEM}}(I, Q, T_H) + R_S[Q + U(I, Q, T_H)I]. \quad (6)$$

The functions  $\Delta T_{\text{TEM}}(I, Q, T_H)$  and  $U(I, Q, T_H)$  used in the equation (6) were calculated by the operating characteristics of the thermoelectric module, which were obtained as a result of processing the experimental data using interpolation polynomials. A calculation algorithm is described in the study [8], which in the present study is modified to take into account of the dependence of the operating characteristics of the thermoelectric module on  $T_H$ . The initial parameters of the problem include the values of the temperature drop  $\Delta T_0$ , thermal resistances  $R_T$  and  $R_S$ , the coolant temperature  $T_8$  and current  $I$ . The calculation results in determination of cooling capacity  $Q$ , the coefficient of performance  $\varepsilon$ , power supply voltage  $U$ , the temperature drop  $\Delta T_{\text{TEM}}$  and the temperature of the hot side of the thermoelectric module  $T_H$ . The calculations had the average values of thermal resistances  $R_T = 0.29$  K/W and  $R_S = 0.11$  K/W specified.

The computationally-obtained dependences  $Q(I)$ ,  $\varepsilon(I)$  and  $\Delta T_{\text{TEM}}(I)$  are marked in Fig. 7 by solid lines. Besides, lower lines of the cells of Table contain numerical values

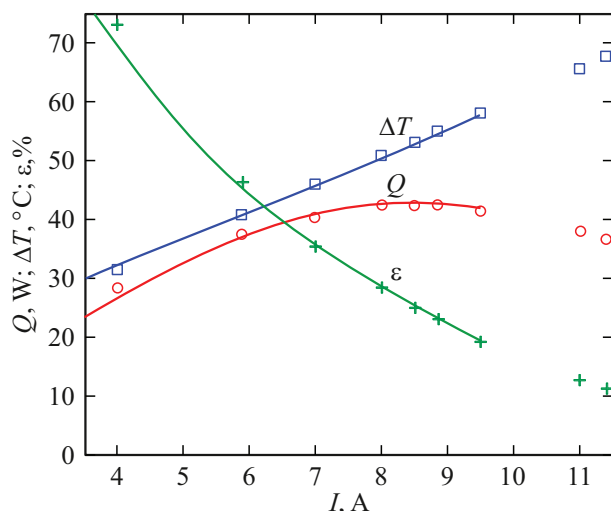


**Figure 7.** Measured values and the calculated dependences of cooling capacity, the coefficient of performance and the temperature drop on the current.

of these parameters for the current values, at which the experiments were performed. These dependences are determined in the smaller current range as compared to the experiments due to boundedness of the ranges of  $I$  and  $T_H$ , for which the TEM operating characteristics were measured. The calculated dependence  $Q(I)$  has a maximum of 42.8 W at the value  $I = 8.5$  A. At the higher current, there is reduction of cooling capacity and, especially, the coefficient of performance. Therefore, these modes are of no practical interest. Generally, the results of the calculations of the characteristics of the thermoelectric cooler model correspond to the experimental data. The largest discrepancy in the numerical values is observed when  $I = 4$  A, which is due to the largest deviation of  $R_T$  and  $R_S$  from their average values used in the calculations. Thus, the results of the measurements of the TEM operating characteristics and their subsequent processing are a basis for numerical analysis of efficiency of the thermoelectric cooling system within the wide range of the temperature conditions.

## Conclusion

The data of the measurements in air were used to determine the operating characteristics of the thermoelectric module TV-199-1.4-0.8 and to detect their dependences on the hot side temperature within the range of the values  $T_H = 14^\circ\text{C} - 40^\circ\text{C}$ . In this range of  $T_H$ , with the current  $I = 8.85$  A, maximum cooling capacity of this commercial TEM varied from 141 to 162 W, while the maximum temperature drop varied from  $64^\circ\text{C}$  to  $72^\circ\text{C}$ . The maximum cooling capacity of the thermoelectric cooler model is recorded in the current range  $I \approx 8 - 9$  A. By means of the numerical model that uses the TEM operating characteris-

tics and takes into account influence of the temperature of the hot side of the thermoelectric module, we have obtained the basic parameters of the thermoelectric cooler model. The results of the calculations agree with the data of the measurements.

Thus, the study has investigated influence of the temperature of the hot side of the thermoelectric module in air, which in real conditions of operation can significantly affect the characteristics of the thermoelectric cooling process. Influence of this factor shall be taken into account when designing and operating the thermoelectric systems of cooling and thermal control.

## Conflict of interest

The author declares that he has no conflict of interest.

## References

- [1] D. Zhao, G. Tan. *Appl. Thermal Engineer.*, **66** (1–2), 15 (2014). DOI: 10.1016/j.applthermaleng.2014.01.074
- [2] Y.W. Chang, C.C. Chang, M.T. Ke, S.L. Chen. *Appl. Thermal Engineer.*, **29** (13), 2731 (2009).
- [3] M.Yu. Shtern, Yu.I. Shtern, A.A. Shevchenkov. *Izvestiya vuzov. Ser. Elektronika*, **4**, 30 (2011) (in Russian).
- [4] N.P. Semena. *Thermophys. Aeromechan.*, **20** (2), 211 (2013). DOI: 10.1134/S0869864313020078
- [5] T.A. Ismailov, O.V. Yevdulov, N.A. Nabiev, S.G. Magomedova. *Biomed. Eng.*, **54** (1), 56 (2020). DOI: 10.1007/s10527-020-09973-7
- [6] O.V. Evdulov, A.M. Ibragimova, Z.M. Daiziev. *Izv. vuzov. Priborostroenie*, **67** (7), 615 (2024) (in Russian). DOI: 10.17586/0021-3454-2024-67-7-615-621
- [7] P. Shostakovskii. *Komponenty i tekhnologii*, **12**, 120 (2009) (in Russian).
- [8] E.N. Vasil'ev. *Tech. Phys.*, **62** (1), 90 (2017). DOI: 10.1134/S1063784217010248
- [9] E.N. Vasil'ev, A.A. Sirotinin. *Zhurn. Sibirskogo fed. un-ta. Tekhnika i tekhnologii*, **18** (2), 176 (2025) (in Russian).
- [10] O.A. Gerashchenko. *Osnovy teplometrii* (Naukova dumka, Kiev, 1971) (in Russian).
- [11] N.V. Pilipenko. *Osnovy proektirovaniya kombinirovannykh priemnikov teplovogo potoka* (Un-t ITMO, SPb., 2016) (in Russian).
- [12] S.Z. Sapozhnikov, V.Y. Mitiakov, A.V. Mitiakov. *Tech. Phys.*, **49** (7), 920 (2004). DOI: 10.1134/1.1778869
- [13] Yu.V. Dobrov, V.A. Lashkov, I.Ch. Mashek, A.V. Mityakov, V.Yu. Mityakov, S.Z. Sapozhnikov, R.S. Khoronzhuk. *Tech. Phys.*, **66** (2), 229 (2021). DOI: 10.1134/S1063784221020109
- [14] V.M. Popov. *Teploobmen cherez soedineniya na kleyakh* (Energiya, M., 1974) (in Russian).
- [15] S.Y. Mesnyankin, A.G. Vikulov, D.G. Vikulov. *Physics-USpekhi*, **52** (9), 891 (2009).
- [16] E.N. Vasiliev. *Zhurn. Sibirskogo fed. un-ta. Tekhnika i tekhnologii*, **18** (4), 440 (2025) (in Russian).

Translated by M. Shevelev